Nitrogen-vacancy center in diamond: Model of the electronic structure and associated dynamics

N. B. Manson, J. P. Harrison, and M. J. Sellars
Laser Physics Center, Research School of Physical Sciences and Engineeering, Australian National University, Canberra, Australian Capital Territory, 0200, Australia
(Received 28 May 2006; published 21 September 2006)

Symmetry considerations are used in presenting a model of the electronic structure and the associated dynamics of the nitrogen-vacancy center in diamond. The model accounts for the occurrence of optically induced spin polarization, for the change of emission level with spin polarization and for new experimental measurements of transient emission. The rate constants given are in variance to those reported previously.

DOI: 10.1103/PhysRevB.74.104303 PACS number(s): 78.47.+p, 78.55.−m, 76.30.Mi

I. INTRODUCTION

Since the nitrogen-vacancy (NV) center in diamond has been detected at a single site level[1–3] the center has attracted attention for various quantum information processing applications. For example, the center has been used as a single photon source for quantum cryptography[4,5] and work in this area has included impressive demonstrations.[6] Another area of interest results from the center having a nonzero spin ground state. The ground state spin can be the qubit and the optical transitions utilized for readout and for qubit manipulation in quantum computing applications. There are again impressive demonstrations in this area.[7–11] With these successes and additional programs under development it might be expected that the properties of the NV center are well understood. However, this is not the case. Despite the extensive publications the center is not well understood and the literature contains many inaccuracies. The purpose of this paper is to revisit our knowledge of the nitrogen-vacancy center, provide an account of the electronic energy levels and explain the dynamics of the center under optical excitation.

II. NITROGEN-VACANCY CENTER

The NV center occurs in diamond containing single substitutional nitrogen when irradiated and annealed.[12,13] Electron irradiation with energies greater than 200 keV creates vacancies.[14] The vacancies are mobile at 800 °C and can become trapped adjacent to the nitrogen impurities. The nitrogen-vacancy complex formed has a strong optical transition with a zero-phonon line at 1.945 eV (637 nm) accompanied by a vibronic band at higher energy in absorption and lower energy in emission. The zero-phonon line has been studied by Davies and Hamer.[13] They have studied the effect of uniaxial stress and from the splitting and polarization they established that the transition is associated with an orbital A-E transition at a site of trigonal symmetry. The trigonal symmetry is consistent with an adjacent nitrogen-vacancy pair with C_{3v} symmetry. In other studies using optical excitation Loubser and van Wyk detected electron spin resonance (ESR) signals of a spin polarized triplet ($S=1$).[15] The ESR they observed was associated with a center having trigonal symmetry and the magnitude of the optically induced signal was found to vary with wavelength in correspondence with the strength of the A-E optical transition. Hence, the center was attributed to the same nitrogen-vacancy complex. With an integer spin ($S=1$) the center must have an even number of electrons and it is taken that the neutral nitrogen-vacancy complex with five electrons has acquired an additional electron from elsewhere in the lattice, probably from another substitutional nitrogen atom. There will then be six electrons occupying the dangling bonds of the vacancy complex.[15] Loubser and van Wyk proposed that the spin polarization arises from a singlet electronic system with inter-system crossing to a spin level of a metastable triplet. However, it was established from hole burning,[16] optically detected magnetic resonance,[17] ESR,[18] and Raman heterodyne measurements[19] that the triplet is the ground state rather than a metastable state. Therefore, their model has to be modified to give a ^3A ground state and a ^3A-^3E optical transition. The optically induced spin polarization can still arise from intersystem crossing and an account is given in this paper.

The six electrons occupy the dangling bonds associated with the vacancy complex. A discussion of this situation is included in a treatment by Lenef *et al.*[20] Although they did not adopt the six electron model[21] they did give a very useful general treatment including the six electron situation and their presentation allows the present discussion to be brief and more descriptive. The dangling bonds are formed from sp^3 orbitals of the carbon and nitrogen atoms and in a vacancy approximating T_d symmetry these can be combined to form a_1 and t_2 molecular orbitals with A_1 and T_2 symmetry, respectively.[22] From symmetry and charge overlap considerations the a_1 is considered to be lower in energy and the t_2 higher. With six electrons $a_1^2t_2^4$ will be the lowest energy configuration and this can also be described as a t_2^2 hole system. When one of the neighboring carbons is replaced by a nitrogen the T_d symmetry will be lowered to trigonal and the t_2 orbital will be split to give, in C_{3v} notation, an a_1 and e orbital. The e hole is lower in energy and, hence, the lowest energy configuration will be e^2, next lowest ea_1 and the a_1^2 highest. The spin-orbit wave functions for the e^2 configuration give $^3A_2$, $^1A_1$, and ^1E states and the ea_1 configuration ^3E and ^1E states. The a_1^2 gives an $^1A_1$. The optical transition is associated with triplets and so the ground state is attributed to the $^3A_2(e^2)$ state and the excited state to the $^3E(ea_1)$ state. There are singlets $^1A_1(e^2)$ and $^1E(e^2)$ and $^1E(a_1e)$ which could lie in the same energy range as the triplets. The $^1A_1(a_1^2)$ lies higher. It has been assumed that the $^1A_1(e^2)$ lies between the triplets and the present treatment accepts this assertion

and will be shown to be consistent with observation. The possibility of intermediate ^1E level(s) will be discussed.

The energy V of each state $^3A_2$, ^3E, $^1A_1$ is determined by the above bonding considerations and the Hamiltonian including spin-orbit V_{SO} and spin-spin V_{SS} interaction is given by

$$H = V + V_{SO} + V_{SS}. \tag{1}$$

Spin-orbit and spin-spin interactions do not affect the degeneracy of the singlets whereas the spin degenerate ground state is only affected by spin-spin interaction normally written as

$$V_{SS} = \rho S_z^2 + \rho'(S_x^2 + S_y^2), \tag{2}$$

where ρ and ρ' are the axial and nonaxial coefficients. The interaction splits the ground state into a singlet $|A_2, S_z\rangle$ with symmetry A_1, and doublet $|A_2, S_x\rangle$, $|A_2, S_y\rangle$ with symmetry E. The spin states $|S_z\rangle$ and $(|S_x\rangle, |S_y\rangle)$ are not mixed.

The ^3E state are affected by both terms. V_{SO} has the form

$$V_{SO} = \lambda(L_z S_z) + \lambda'(L_x S_x + L_y S_y), \tag{3}$$

where λ and λ' are the coefficients associated with the axial and nonaxial spin-orbit interactions. The axial $\lambda(L_z S_z)$ spin-orbit interaction splits the ^3E spin triplet into three twofold degenerate states E, E', and an (A_1, A_2) pair. Within the ^3E state nonaxial spin-orbit interaction is small and will be neglected at present. As will be discussed shortly spin-orbit can give mixing between adjacent states. This can cause a shifting of levels which can be calculated by including this state in the calculation or by including spin-orbit interaction to second order. The form of this latter term is the same as that of spin-spin interaction. In high symmetry (e.g., T_d) this has the form[23]

$$V_{SS} = \rho[(\underline{L}\underline{S})^2 + 1/2(\underline{L}\underline{S}) + L(L+1)S(S+1)]. \tag{4}$$

In trigonal symmetry one has to allow for the difference in the axial and nonaxial terms. The interaction modifies the separation of the above states but does not change the wave functions and the wave functions are the main interest here. The states and the symmetry adapted wave functions are given in Fig. 1(a). The states with S_z spin projection are not mixed with the spin states with S_x and S_y spin projection. The $^3A_2 \leftrightarrow {}^3E$ transition is orbitally allowed and, as the spin projection is not changed by the electric dipole operator, the optical transitions will be the same strength for each of the spin projections [shown as solid vertical arrows in Fig. 1(a)]. There are no transitions involving a change of spin and it can be concluded that optical cycling of the $^3A_2$-^3E transition will not result in change of spin projection and consequently can not give any spin polarization. This situation does not change when considering vibronic interactions as spin projection is conserved.

Spin-orbit interaction mixes singlets and triplets which transform according to the same irreducible representation. The mixing provides an avenue whereby symmetric vibration can cause a population relaxation between the mixed singlets and triplets. The symmetry considerations, therefore, determine the allowed intersystem crossing and these are also shown in Fig. 1(a). Where there is only a $^1A_1$ singlet level the intersystem crossing is restricted to states that transform as A_1 irreducible representations. There can be excitation of population out of the E ground state level with S_x or S_y spin projection to the A_1 spin-orbit level of the ^3E state. Population in this state can decay via the singlet to the S_z spin projection of the ground state. Such an excitation and decay, therefore, causes a re-orientation of the ground state spin projection and with continuous excitation population can be transferred to the ground S_z spin state. This is consistent with the preferred spin orientation established experimentally.[24] With these selection rules, assuming the optical induced spin polarization is faster than spin-lattice relaxation, the spin polarization would be 100% but this is not what is observed.[25]

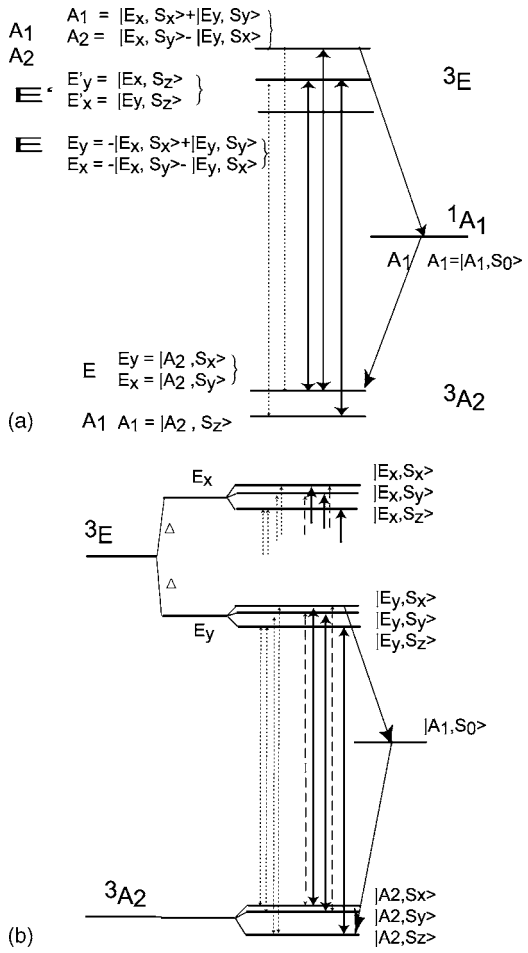

FIG. 1. (a) Energy levels of the NV center in C_{3v} symmetry. The excited state is split by spin-orbit interaction whereas the ground state is split by spin-spin interaction (not shown to scale). The figure gives the symmetry adapted wave-functions. The solid arrows indicate the spin-allowed optical transitions. The dashed arrows indicated weak transitions which are allowed through the mixing of the $(^3E)E$ and $(^3E)E'$ basis states by transverse spin-orbit interaction. The diagonal arrows give intersystem crossing allowed by spin-orbit interaction. (b) Energy levels and wave functions of the NV center in the presence of a strain field. The wave functions are appropriate for a strain field perpendicular to a reflection plane. The transitions are derived from those allowed in (a).

The extra consideration is the nonaxial λ' $(L_xS_x+L_yS_y)$ spin-orbit interaction which we have previously neglected. This spin-orbit term causes a mixing of the two ^3E states (denoted E and E') transforming as an E irreducible representation. These states have different S_z and S_x,S_y spin projections and, hence, the mixing gives rise to optical transitions that do not conserve spin (dashed arrows in Fig. 1). The transitions are observed in hole burning spectra[16,26–31] and are the transitions that limit the degree of spin polarization. It is anticipated that the strength of the nonaxial spin-orbit interaction is small. This is concluded from consideration of the one electron operators. Spin-orbit interaction will be isotropic for t_2 orbits in T_d symmetry but the axial contribution is quenched when the orbit is split into twofold degenerate and nondegenerate states. In C_{3v} the nonaxial spin-orbit interaction between the individual twofold degenerate states is formally allowed but its contribution arises from higher order effects. The nonaxial spin-orbit interaction is, therefore, anticipated to be small and the nonspin conserving optical transitions will be weak. Although weak the transitions play an important role in limiting the degree of spin polarization.

We briefly consider the situation where a ^1E state(s) lies between the $^3A_2$ and ^3E. If this were the case there could be symmetry allowed relaxation from the excited triplet $(^3E)E$ and $(^3E)E'$ states to such an intermediate ^1E singlet state. However, using the two hole description the relaxation is found to be forbidden in the case of the triplet $(^3E)E'$ state [cancellation of terms for a $^1E(a_1e)$ and forbidden for one electron operators for $^1E(e^2)$ states] implying that there will still not be population transfer out of states with S_z spin projection. There can be relaxation from the other triplet $(^3E)E$ state involving the S_x,S_y spin projections to a ^1E level. Given that there is also an intermediate $^1A_1$ there can be two alternate situations depending on the ordering of the $^1A_1$ and ^1E singlet levels. Should the ^1E state lie lowest the decay will be to the $(^3A_2)E$ component of the ground state. This state has a S_x,S_y spin projection and the optical cycling will have had no consequence implying no change in spin orientation. However, if the ^1E state lies above the $^1A_1$ level there will be radiative (or nonradiative) decay to the lower singlet level, the $^1A_1$, followed by the relaxation, as discussed in the previous paragraph, to the S_z spin projection of the ground state. This process will lead to the same spin change and spin polarization as before. The simple consequence of involving the ^1E singlet is that the total ($^1A_1$ plus ^1E) spin polarization process will be more efficient. Thus, if there is an intermediate ^1E state, to be consistent with observation it must lie at an energy higher than the $^1A_1$ state. It is recognized that this order is in disagreement with calculated energy levels.[32] However, there is an appeal of including a higher single ^1E state as it could lie close to the excited triplet level and the $^1A_1$ close to the ground state thus accounting for the relatively fast intersystem crossing reported below. However, there is no fundamental difference in the dynamics and it is sufficient in this work to restrict the discussion to one singlet level $^1A_1$.

It is common for there to be strain in diamond and it is worth considering the consequence to the energy levels and the associated dynamics. There will be no fundamental change with axial strain as all it gives is a uniform shift of the energy levels and no change of the wave functions or the dynamics. However, the component of the strain at right angles to the axis of the center lowers the symmetry and the extra crystal field lifts the orbital degeneracy of the excited state to give two orbital nondegenerate states denoted E_x and E_y.[20] We consider the case where this strain splitting is larger than the spin-orbit interaction. Where the strain retains a reflection plane the Z,X,Y axes will be determined by symmetry. The wave functions for this situation are as given in Fig. 1(b). The diagonal spin-orbit interaction is quenched and the order of states (same in both optical components) are determined by spin-spin interaction. In the limit of small nonaxial spin-orbit interaction there is still little mixing of the S_x,S_y spin states with the S_z spin states. The transitions and intersystem crossing can be determined from the parent state and are shown in Fig. 1(b). The spin allowed transitions will have near the same strength as in the zero strain case but they are now totally polarized. The only minor change is loss to the dashed transitions between the states with different S_x and S_y projections. These arise where the strain is not sufficient to totally quench the effect of the diagonal spin-orbit interaction. A more significant effect is in the strength of the nonspin-conserving transitions induced by nonaxial spin-orbit interaction. They will become significantly stronger as the separation of the S_z and (S_x,S_y) is reduced and the mixing increased. When the strain does not retain reflection symmetry the effective X and Y axis may be different between ground and excited states and all transitions and intersystem crossings will become allowed in principle (no symmetry restrictions). However, the selection rules will be dominated by those allowed in zero order and the perturbation approach in Fig. 1(b) is anticipated to give a reasonable approximation to the dominant excitation and decay channels.

Which of the diagrams, Figs. 1(a) or 1(b) (or an intermediate case), is appropriate for a given center depends on the relative magnitude of the stress, spin-orbit, and spin-spin interaction. Spin-orbit for the carbon atom is known to be a few cm^{-1} ($\sim$200 GHz) and a spin-orbit splitting of 1 cm^{-1} (30 GHz) was obtained for the ^3E state from optical magnetic circular dichroism measurements.[16] This value maybe marginally high as an optical line width of 15 GHz has been reported recently for small ensembles within single crystals of diamond[29] and there is an indication that spin-spin interaction may also contribute to the line width. Santouri *et al.*[29] have also shown, using two-laser hole burning experiments, that for even a small strain splitting of 10 GHz the energy scheme is equivalent to Fig. 1(b). As strain splitting is usually much larger ($>$100 GHz) it is taken that this energy scheme will be typical of centers in an ensemble sample as used here.

The dynamics associated with optical excitation can be determined without detailed knowledge of the excited state energy levels. This is because from the above discussion it can be seen that the system can be reasonably quantized by its spin projection S_z or (S_x,S_y) and this is not altered by stress. The dynamics are largely determined by the crossing between these two spin projections and the symmetry considerations give the two main mechanisms. The changes of

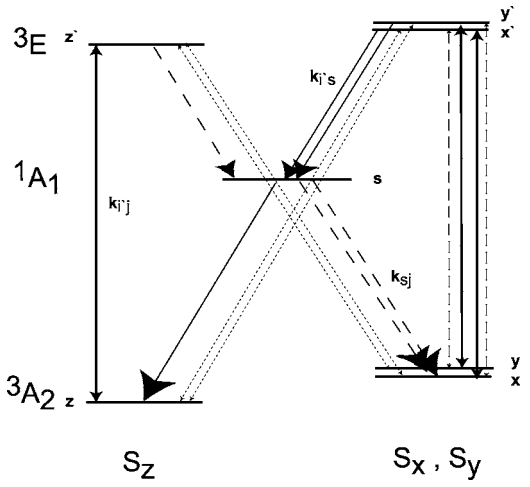

FIG. 2. Energy levels for a perturbed NV center. The significant energy levels of Fig. 1(b) are redrawn to highlight the inter-system crossing. All the radiative and nonradiative transitions are shown. The allowed transitions considered in the text are shown by solid arrows. The dashed vertical arrows on the right are allowed but can be taken to be zero for present experiments. Also the intersystem crossing indicated by the dashed arrows are zero in first order.

spin are through the intersystem crossing via the singlet and through the weak non-spin-conserving optical transitions. The effective energy scheme is given in Fig. 2, where the S_z states are shown on the left and the (S_x, S_y) on the right. The singlets are drawn centrally. Spin polarization involves displacement of population from the states on the right to the states on the left. The transitions including those that change the spin projection are shown as solid lines as determined by the parent states in C_{3v} symmetry. For completeness other transitions allowed in low symmetry are shown as dashed lines. The low symmetry situation is similar to that proposed by others[10,33,34] and to assist comparison we adopt their shortened notation. The ground spin states are defined as x, y, and z; the excited triplet states as x', y', and z' and the singlet level as s. In the following experiments we determine the values of the parameters using bulk samples.

III. EXPERIMENTAL DETAILS

Several type 1b diamonds were used in these studies. They were irradiated with energetic electrons (> MeV) and annealed. The nitrogen-vacancy concentrations varied from 3×10^{18} per cm^3 to 10^{17} per cm^3 and there was no indication that the dynamics of the optical cycle varied significantly for concentrations in this range.

The experiments involve transient and CW excitation studies using a frequency doubled Nd:YAG laser. The excitation wavelength is 532 nm which is near the peak of the $^3A_2 \leftrightarrow {}^3E$ absorption band. The emission was detected by a S-20 photomultiplier or pin diode with a response time of 30 ns. With the exception of the measurement of the spectrum the emission wavelength detected was selected using absorptive filters.

The studies involved three different excitation and detection geometries. For low level excitation the intensity was

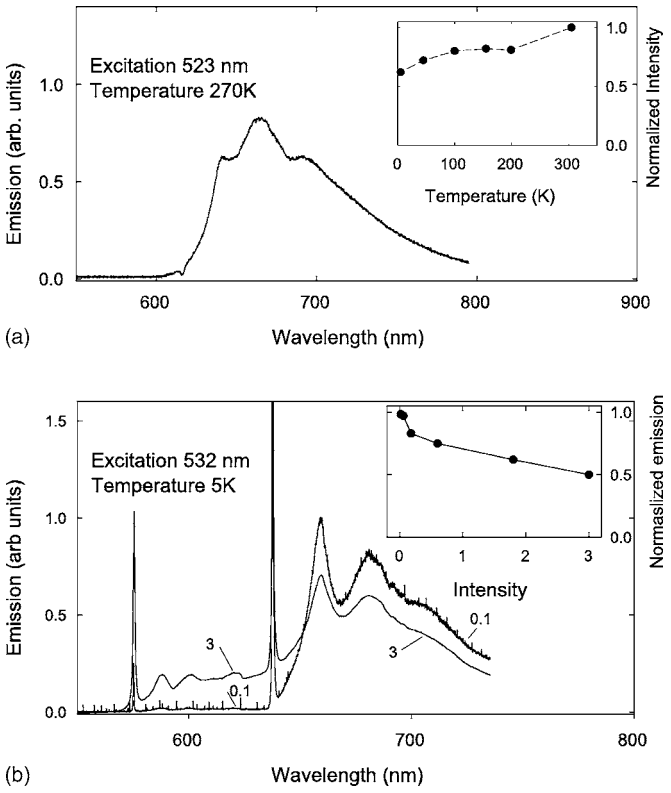

FIG. 3. Spectral characteristics of the NV center. (a) Emission spectra of a diamond containing a high concentration of NV centers measured near room temperature using low excitation densities of 1 W/cm^3. Inset: the variation of the NV emission at 666 nm as a function of sample temperature (b) Low temperature emission spectra of the NV center measured with various excitation densities (from Ref. 36). Inset: variation of NV emission intensity as a function of excitation energy density (units of 1×10^5 W/cm^3). Emission normalized to excitation intensity.

determined from the laser power and the beam diameter. The emission at 45° was focussed on the pin diode. For high intensity measurements a confocal arrangement with an oil immersion objective was used. The excited diameter was 0.2 micron with the emission spot focussed onto a pinhole. A 1 mW beam gave an estimated power density of 2×10^6 W/cm^2. With the small excitation and detection volumes the signals were weak and long collection times were required to obtain satisfactory signal to noise ratios. The majority of the measurements were taken with a third geometry where satisfactory signals could be obtained more rapidly. The light was focused with a microscope objective and the back emission collected by the same objective. For the same laser power the intensity at the sample was approximately two orders of magnitude lower than that obtained with oil immersion objective and it required a 100 mW laser beam to obtain a maximum intensity of 2×10^6 W/cm^2. The unsatisfactory feature of this geometry is that the intensity was not constant over the collected volume.

At low intensities where slow (>ms) responses were obtained the light was gated with a mechanical chopper whereas for the fast speeds associated with the high intensities the light was gated using two acousto-optic modulators

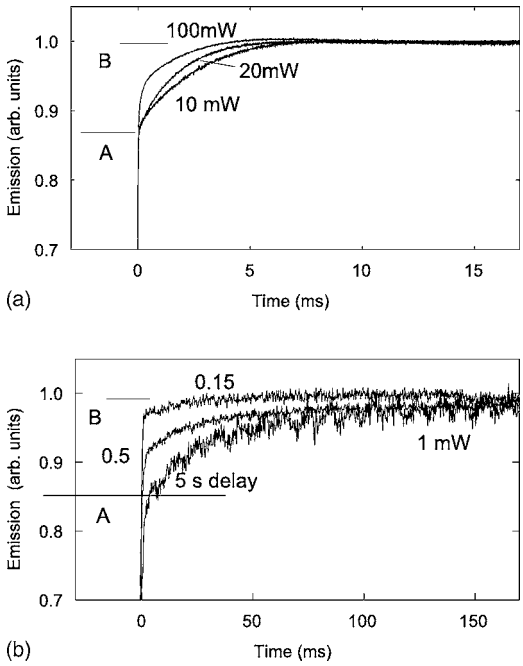

FIG. 4. Emission obtained when gating on excitation at time 0. The excitation is at 532 nm and is gated with a mechanical shutter. (a) Response for various laser powers; 10 mW corresponds to an intensity of 1 W/cm^2. The emission increases to an initial value A, 86% of its final value. The rate of increase of the emission to its final CW value B depends on intensity of excitation. The sample has a spin-lattice relaxation time of 100 ms and sample held in dark for 500 ms prior to excitation. (b) Responses for various periods in the dark. For these traces the sample is cooled to 100 K and the spin-lattice relaxation time is increased to 500 ms.

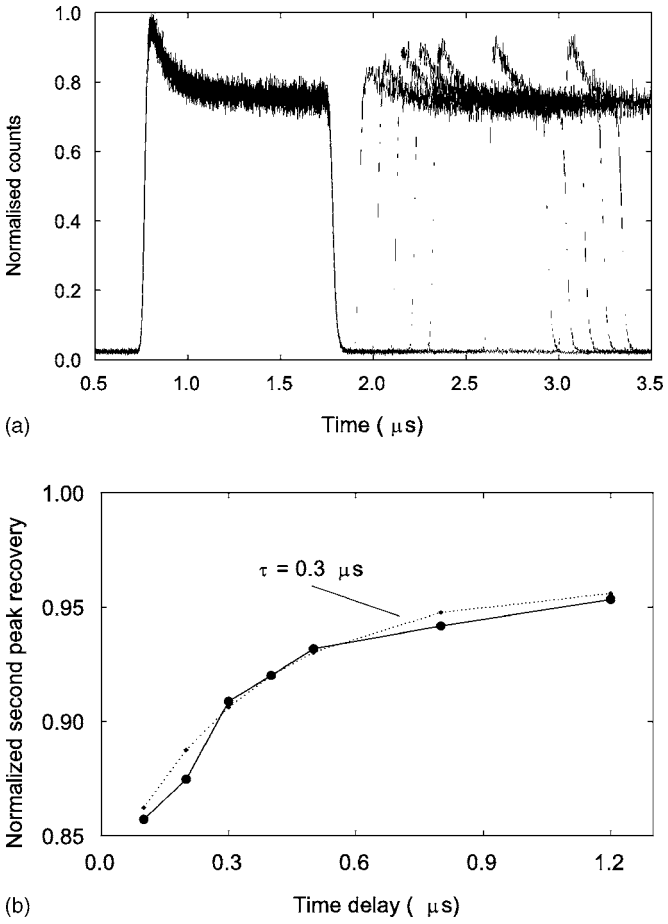

FIG. 5. Emission response to a double light pulse each 2 μs separated by a delay which is varied. (a) The emission is shown with various delays between the two pulses. The responses for the first pulses all overlap whereas the second pulse is delayed by the dark period. The peak associated with the second pulse recovers with the dark period and the height of this pulse is plotted in (b) as a function of the duration in the dark. The dashed curve illustrates the response for a 0.3 μs recovery rate. The repetition rate of the pulse pair was 10 kHz. The intensity of the excitation was 3×10^6 W/cm^2.

in series. The rise time of the A-O modulators is 30 ns. When gating off there was a weak component that lasted for a μs. However, no measurements were taken when gating the light off.

A. Preliminary measurements

The emission of the NV center has been reported on many occasions. The general characteristics are shown in Fig. 3. Near room temperature the emission gives a band stretching from 630 to 800 nm with vibrational structure and a weak zero-phonon line at 637 nm [Fig. 3(a)]. Cooling has little effect on the vibronic absorption band[35] and consequently there is little change in the amount of light absorbed from the laser beam when using an excitation wavelength within the vibronic band. Consistent with this, the total emission does not show a significant change when the temperature is lowered [inset in Fig. 3(a)]. The most obvious change in cooling to low temperatures is that the zero-phonon line becomes sharper and more prominent [Fig. 3(b)]. The Huang-Rhys factor is 3.7 with only 2.7% of the transition strength being associated with the zero-phonon transition.[35] At high excitation densities there can be photoionization of the NV center of interest and the creation of the neutrally charged $[NV]^0$ center.[36,37] This center has a zero-phonon line at 575 nm with a vibronic band to lower energy.[38] The increased contribution of this center at high intensities is illustrated in Fig. 3(b).

As discussed earlier the NV center exhibits optically induced spin polarization of the ground state triplet and there is a change of the emission intensity associated with this polarization (no change in absorption). The change is illustrated in Fig. 4. In the dark the sample becomes unpolarized and when excited the emission has an initial intensity level A. After exciting for a period the sample becomes polarized and the strength of the emission increases to a second value B [Fig. 4(a)]. The rate at which the emission increases from the level A to B is linearly dependent on the excitation intensity. Should the sample be in the dark for a period less that the spin-lattice relaxation time (T_1) the initial emission level will be at a value between A and B and varying the dark period varies this level. This variation of emission level with the duration in the dark can be used to establish the spin lattice relaxation time and measurements of this type are shown in Fig. 4(b). The A/B ratio is of considerable interest. To ensure

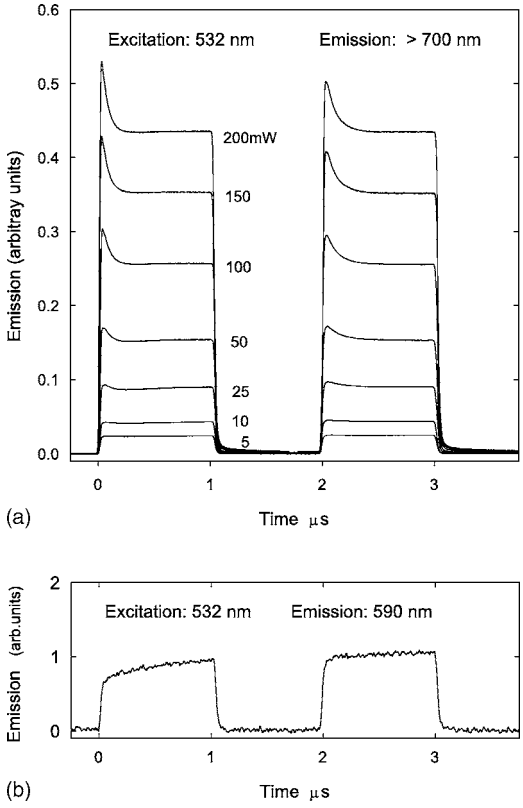

FIG. 6. Emission of the NV center for a pair of square wave excitation pulse of light at 532 nm. The light is focused with a microscope objective and for 100 mW the intensity is 2×10^6 W/cm^2 The back scattered emission is detected using a (a) 700 nm long pass filter, (b) 100 nm band pass filter at 590 nm.

a satisfactory A measurement it is necessary to have the sample in the dark for a period long compared to T_1 whereas to obtain the saturation value B the intensity has to be sufficient to obtain the higher emission level within a time short compared to T_1. A decrease of the spin polarization through spin diffusion must also be avoided. When meeting these conditions the A/B ratio is 0.86 ± 0.02.

B. Dual pulse measurements

The sample is excited with two intense excitation pulses and the delay between two pulses is varied. These measurements utilized the confocal arrangement with oil immersion and intensities of 10^6 W/cm^2. The repetition rate was 10 kHz. The results are shown in Fig. 5(a). In the figure the response associated with the first pulse of every pair is overlapped whereas the emission associated with the second pulse is displaced as the delay between the pulses is varied. Every pulse exhibits an initial peak followed by a decay within a μs to a lower level. For the first pulse the magnitude of the peak is 1/3 that of the equilibrium signal. When the light is gated off the sample has to remain in the dark for a period before the second pulse gives a peak and the magnitude of the peak increases as the duration of the dark period is increased. This recovery has two components and the faster recovery is shown to have a response time of 0.3 μs

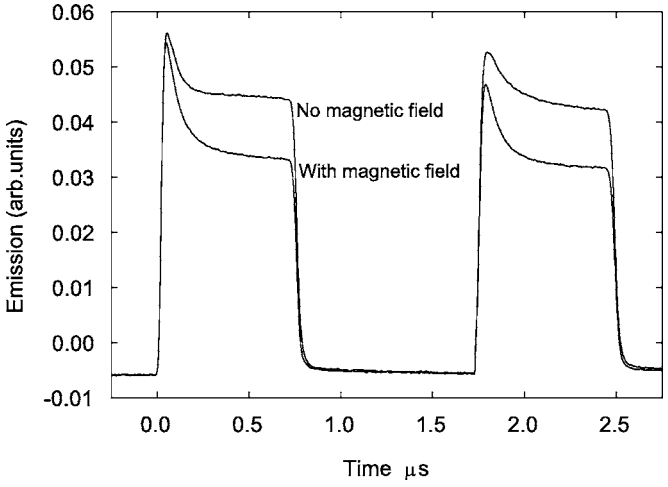

FIG. 7. Emission of the NV center for a pair of square wave excitation pulses of light at 532 nm with laser intensity of 100 mW. No magnetic field is applied in the case of the upper trace and corresponds to the 100 mW trace in Fig. 6. For the lower trace a field of 500 G is applied in a random direction (not aligned with an axis of any center).

[Fig. 5(b)]. There is a slower recovery over the 100 μs between pulses and we will comment on this slower recovery later.

For the second series of measurements the emission is obtained for a pulse pair of 1 μs duration separated by 1 μs but with long delays between the pulse pairs. The measurements were made using the alternate geometry where the excitation and detection involved a larger but less well defined volume. The period between pairs (>10 ms) was chosen to be much larger than ground state spin-lattice relaxation time T_1 (1 ms). The intention is for the system to be unpolarized at the start of the first pulse but polarized at the start of the second pulse. Figure 6(a) shows the results of the emission response for pulse pairs for laser powers from 5 to 200 mW corresponding to estimated intensities of 10^5 W/cm^2 to 4×10^6 W/cm^2. The emission is restricted to longer wavelengths (>700 nm) to avoid including emission from $[NV]^0$ centers. The emission of the $[NV]^0$ center by itself was also obtained by detecting the emission at 590 nm using a narrow band filter. This emission is shown in Fig. 6(b).

The responses in Fig. 6(a) show peaks at the start of each pulse and the magnitude increases with intensity. The peak height of the second pulse is consistently several percent lower than that of the first. Also the decay rates are different for the two pulses, the first being faster than the second.

The effect of applying a weak magnetic field of a few hundred gauss was also recorded. The response to a pair of intense (100 mW) excitation pulses at 532 nm were measured both with and without the magnetic field applied in a random direction (Fig. 7). In comparing the two traces there are three significant differences. The first emission peak is almost the same for the two traces but the subsequent decay is to a much lower level when the magnetic field is applied. With the second pulse there is a significant difference in the peak heights, being lower with the field is applied. Also with

the second pulse the decay to the lower level is faster when the magnetic field is applied.

IV. RELAXATION AND INTERSYSTEM DECAY RATES

The dynamics scale with the lifetime of the excited state and various values have been reported in the literature. Collins *et al.*[39] have obtained values of 12.9±0.1 ns for a natural diamond and 11.6±0.1 ns for a synthetic diamond. Lenef *et al.*[20] has also obtained a measure of 12.96±0.14 ns obtained in relation to photon echo measurements. A value of $\tau = 13$ ns is adopted here. The radiative rate constants are, hence, $k_{x'x}=k_{y'y}=k_{z'z}=77\times10^6$ s^{-1}. (The present experiments are not sensitive to the dashed vertical transitions in Fig. 2 between the x,x' and the y,y' states and the associated rate constants can be taken to be zero, i.e., $k_{xy'}=k_{yx'}=0$.) It is noted that the present model indicates that there should be two components to the emission decay associated with excited states, one with z' and one with x',y'. The emission from the z' excited state has the slower decay rate and dominates when the system is spin polarized, perhaps explaining why the two values (differing by only 30%) have not been detected. Two components of 9 and 2 ns have been observed by Hanzana *et al.*[40] but the measurements are inconsistent with previous values. These lifetimes require further investigation.

The increase in emission from a level A to a level B can be used to establish the fraction of the population transferring into the singlet. For example the 14% emission change between having all the population in the z spin ground state and having the population evenly distributed between the three spin states implies 27% of the population from each of the x',y' excited spin states transferring nonradiatively to the singlet s. This has to be increased to 39% to allow for the incomplete spin polarization reported below. The intersystem crossing rates are then $k_{x's}=k_{y's}=30\times10^6$ s^{-1}. In correspondence with the model, the intersystem crossing from the z' state to the singlet is taken to be zero and, hence, $k_{z's}=0$.

For the low intensities no population is maintained in the singlet. This is changed at high intensities and the transient emission displays different characteristics. With population being stored in the singlet level there is a drop in emission and this is observed in all of the two-pulse experiments (Figs. 5–7). There will be no initial peak if the excitation is gated on and off within a few ns as there will be no change in the singlet population. The recovery of the peak requires a period in the dark (Fig. 5) and the time required corresponds to the rate at which population decays from the singlet to the ground state. The value of the singlet lifetime obtained from this peak recovery is 0.3 μs and this gives $k_{sz}=3.3\times10^6$ s^{-1}. As in the model we take $k_{sx}=k_{sy}=0$.

In a recent paper we have reported that the maximum spin polarization obtained for an ensemble under continuous excitation is 80%.[25] This means that the probability of optically transferring spin projection from the z spin state to an x,y spin is 1/4 of the above process giving rise to the spin polarization. The mechanism is attributed to the nonspin conserving optical transitions (diagonal arrows between triplet levels in Fig. 2) and implies that the rate constants are $k_{zx'}=k_{zy'}=k_{xz'}=k_{yz'}=1.5\times10^6$ s^{-1}. Loss of spin polarization could also arise from the reverse inter-system crossing via the singlet level. However, the model predicts that the rate is zero, $k_{z's}=0$ and, as given previously, the decay from the singlet to the x and y ground states are also zero.

Rates	Units 10^6 s^{-1}
$k_{xx'}=k_{yy'}=k_{zz'}$	77
$k_{xy'}=k_{yx'}$	0
$k_{x's}=k_{y's}$	30
$k_{z's}$	0
k_{sz}	3.3
$k_{sx}=k_{sy}$	0
$k_{zx'}=k_{zy'}=k_{xz'}=k_{yz'}$	1.5

V. RATE EQUATIONS

In the previous section estimates of the parameters of the model in Fig. 2 have been obtained from simple experimental observations. By adopting these parameters we can determine the populations and the emission for any optical field by solving the classical rate equations

$$dn_i/dt = \Sigma_j(k_{ji}n_j - k_{ij}n_i), \tag{5}$$

where n_i is the population of level i $(i=z,x,y,z',x',y',s)$, and k_{ij} gives the rate for the $i\rightarrow j$ transition. The significant parameters associated with the optical transitions are

$$(k_{z'z},k_{x'x},k_{y'y}),\quad (k_{x'z},k_{y'z},k_{z'x},k_{z'zy}),\quad (k_{x'y},k_{y'x}), \tag{6}$$

where the values within brackets are equal in first order. The related optically driven terms are obtained by setting $k_{ij}=k^*k_{ji}$, where k indicates the strength of the optical pumping. $k=1$ corresponds to the case where the optical pumping rate of the allowed transitions equals the emission decay rates. The inter-system crossings are determined by the rates

$$(k_{z's}),\quad (k_{x's},k_{y's}),\quad (k_{sz}),\quad (k_{sx},k_{sy}). \tag{7}$$

There are no reverse terms associated with the intersystem crossing and, hence, the related parameters with the indices reversed are zero. Likewise all the relaxation rates between the spin levels z, x, and y and between levels z', x', and y' are small. These parameters can be considered equal and given a small value but the effects are not significant in the calculated responses.

Where a sample has been in the dark for a period long compared to the spin-lattice relaxation time the population will initially be equally distributed over the three ground state spin levels z, x, and y. Emission is established in a time of the order of the excited state lifetime of 10–20 ns and with continuing excitation the emission level increases as population is transferred to the z state (Fig. 8). This behavior is in correspondence with observation (Fig. 4). However, little significance can be drawn as there has not been an independent measurement of the optical pumping rate and the magnitude of the rise in Fig. 4 has been used in determining the parameters of the system.

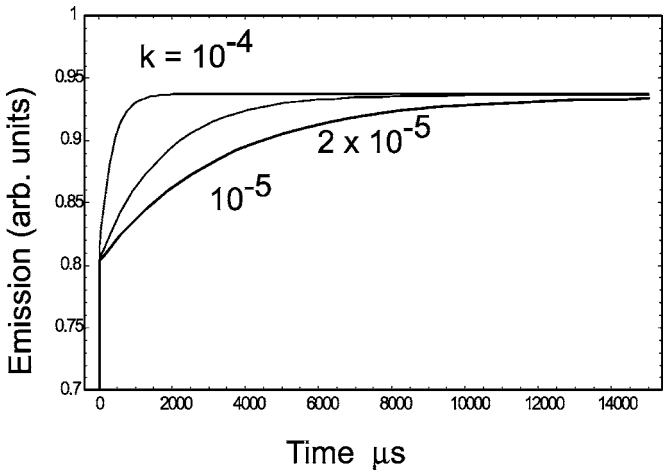

FIG. 8. Emission calculated from solution of the rate equation for energy scheme in Fig. 2. The intensities k are given in units of $1/\tau$. The value of the parameters in units of 10^6 s^{-1} introduced in the text are $k_{zz'}=k_{xx'}=k_{yy'}=77$; $k_{sz}=3.3$, $k_{sx}=k_{sy}=0$; $k_{z's}=0$; $k_{x's}=k_{y's}=30$; $k_{zx'}=k_{zy'}=k_{xz'}=k_{yz'}=1.5$.

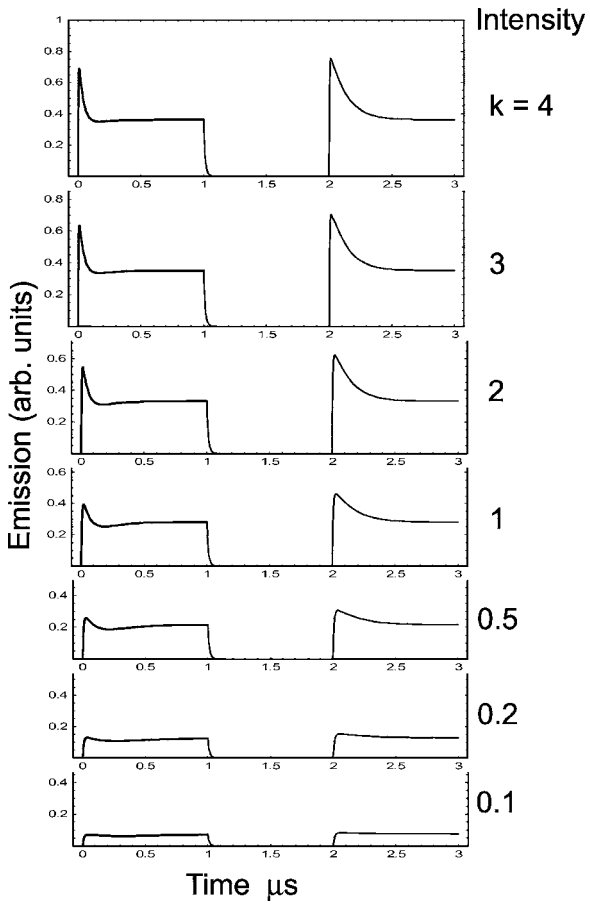

FIG. 9. (a) Emission predicted from the solution of the rate equations for a pair of excitation pulses. The emission is shown for various excitation intensities k shown on the right in units of $1/\tau$. The value of the parameters are given in the text and summarized in the caption of Fig. 8.

Other than the optical pumping rate there are no free parameters when calculating the emission associated with the dual pulses experiments. In these experiments the intensities are high and the transfer of population into the singlet level is initially faster than the relaxation from the singlet to the ground state. Consequently there is a build up of singlet population and associated with this there is a drop in the emission level. The situation is calculated for a light field switched on and held constant for 1 μs, switched off for 1 μ, and then switched on again for a further 1 μs. With the intense excitation the system reaches equilibrium during the 1 μs pulse and so is spin polarized well before the end of the first pulse. In the dark period there is a relaxation of the singlet population but there is no loss in spin polarization. The result is that for the second light pulse the system starts spin polarized with a preferential population in the z spin ground state. In this case the transfer to the singlet is less efficient and the build up of population in the singlet level is slower. This accounts for the observed slower drop in emission intensity with the second pulse. The behavior for representative intensities is shown in Fig. 9.

The results of the calculations can be compared with the experimental measurements of Fig. 6. It should be recognized that the calculations are for a simpler situation than realized experimentally. The calculations are for an ensemble of identical centers with identical optical pumping rates whereas the experiment involves four orientations and variation in the optical pumping rates. The consequence of these factors can be approximated by adding a square wave emission response to the calculated emission response before comparing with experiment. The structured component of the response (the "peak") will then represent a smaller fraction of each pulse. Another important consideration is that photoionization has not been included. In the calculations the peak of the second pulse is stronger than that of the first whereas it is the reverse in the experiment. The difference is due to photoionization. Photoionization causes there to be a reduction in the number of NV centers during the first pulse (giving small alteration to the slope). The recovery is slow and there is no recovery during the short dark period. Hence, the number of centers involved is larger at the start of the first pulse than at the start of the second pulse. When allowing for these factors and recognizing that the parameters have been determined from independent measurements the correspondence between the calculated responses in Fig. 9 and equivalent experimental traces in Fig. 6 is very satisfactory.

VI. MAGNETIC FIELD CALCULATION

A magnetic field other than along the trigonal axis causes mixing of the spin states[15] and consequently with a randomly oriented field the populations are not associated with separate z, x, and y states. The effect can be approximated by retaining equal populations in the three spin projections and the result of doing this is shown in Fig. 10. The upper trace gives the response in the absence of a magnetic field and is the same as in the previous section with $k=1$. For the lower trace the populations in the three ground spin states are equalized. When this is done to approximate the effect of a magnetic field, there is no spin polarization and the responses are the same for the two pulses. With the field ap-

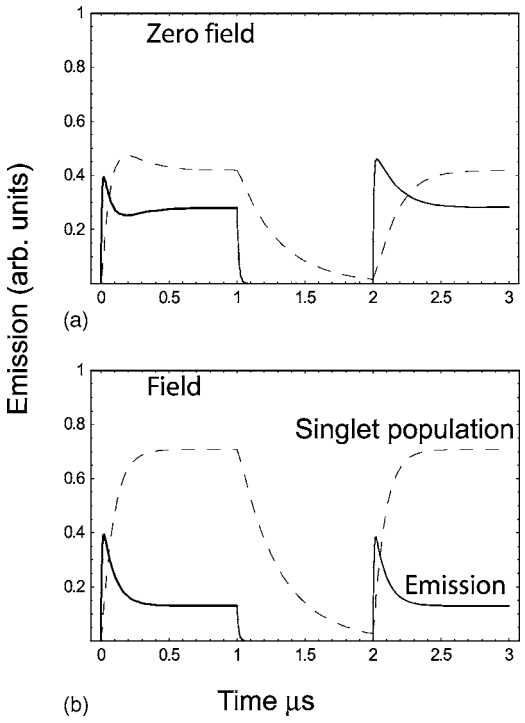

FIG. 10. Emission predicted from solutions of rate equations illustrating effect of an applied magnetic field. The solid line in the upper trace shows the emission of system determined from solution of rate equations for energy scheme as shown in Fig. 2. The dashed line indicates the variation in population of singlet level. For the lower trace the three ground states are mixed, effectively maintaining equal population in the three spin projections. The excitation rate is $k=1$ in units of $1/\tau$. The value of the parameters are given in the text and summarized in the caption of Fig. 8.

plied there continues to be optical excitation from the x,y state and more efficient transfer into the singlet level. The result is that the equilibrium population in the singlet level is higher and less centers contribute to the emission. The final emission is lower and this is what is observed. It should be noted that equivalent effects can be obtained by applying resonant microwave fields to maintain population in the x,y states. At high intensities the drop in equilibrium emission level caused by the microwave field can be much larger[41] than the 14% obtained at low intensities. This is due to the change of the population stored in the singlet level.

In comparing the responses with and without an applied magnetic field there is a variation in the magnitude of the peaks. The peak in the emission associated with the first pulse is similar with and without field. However, the magnitudes associated with the second pulse are very different. As discussed previously, the difference in peak heights between the first and second pulses is due to photoionization varying the number of centers. A smaller second peak indicates that the magnetic field has caused an increase in the photoionization. This can be attributed to the field increasing the population in the excited states (excited triplet plus singlet) and the ionization being out of these states. It is desirable to establish whether the ionization occurs through tunnelling out of these states or is light induced. This requires further investigation.

VII. COMPARISON WITH OTHER WORK

There have been many publications referring to the singlet level in the NV center and many of these publications give information that is in conflict with the current model. The disparities are discussed below.

In the present work it is shown that the singlet has a short lifetime of 0.3 μs. This contrasts with the value of 0.275 s given when the intermediate ^1A singlet was first proposed. Redman *et al.*[18] deduced that a long lived electronic state accounted for a narrow 1.2 Hz resonance observed in a near degenerate four-wave mixing experiment. They recognized that the narrow resonance could be associated with a long lived spin state but their estimates of the spin-lattice relaxation times suggested otherwise. However, a spin-lattice relaxation time of 0.275 s is quite realistic for NV centers in diamond and we consider that this was the correct interpretation. In this case their data can be explained without invoking a long lived singlet state and the information would be consistent with that presented here.

The presence of a long lived singlet has also been adopted in accounting for the loss of emission from single centers as temperature is lowered.[2,3] With excitation it was considered that the singlet becomes populated but there is a thermally stimulated back transfer to the emitting level such that at room temperature there is little loss of emission. The back transfer decreases with lowering temperature and the center can remain in the singlet level for a considerable time resulting in a drop of the average emission intensity. This decrease in intensity occurs for zero-phonon line excitation. However, if the explanation is correct there will be an equivalent loss of emission when the excitation is within the vibronic band. This is not the case. There is little change in NV emission intensity with a lowering of temperature (see Fig. 3). The more likely explanation for the loss of emission in the case of zero-phonon line excitation is spectral hole burning. There are a range of processes (change of spin state, reorientation of center, or movement of charge in the neighborhood of the center) which can shift the absorption frequency and cause a decrease of absorption for a laser held at fixed frequency. With a decrease in absorption there will be an equivalent decrease in emission and the effect will become more pronounced as the temperature is lowered due to narrowing of the homogeneous line width. The decrease in emission is, therefore, attributed to this process and not with populating the singlet level. Clearly no information about the energy of a singlet can be obtained from such experiments.[3,42]

It is often assumed that there is no decay from the singlet to the ground state.[4,5] Should this be the case the spin polarization would have to arise through the back transfer and such a process would be strongly temperature dependent. This is not what is observed. Spin polarization occurs from liquid helium temperatures to room temperatures and in the original measurements of spin polarization Loubser and van Wyk[15] have shown that the polarization is maintained to 500 K. Another more important issue is to question how spin polarization arises with the thermal back transfer process. No details have been presented as to how the spin polarization occurs. This is in contrast with the present model where, rather than back transfer, there is decay from the singlet di-

rect to the ground state. With the decay channels proposed one can readily account for the spin polarization. It can be concluded that the NV center can be understood without back transfer playing a role.

It is noted that the analysis of the photon statistics associated with emission from single NV centers[2–5,33] has assumed that either there is significant singlet-triplet back transfer or a long lived singlet state (or both). Consequently the parameters reported are inconsistent with the values obtained here. Such measurements need to be reanalyzed using the present model and consideration given to contributions associated with photoionization.

Wrachtrup and co-workers at University of Stuttgart and at the National Academy of Sciences of Belarus have presented an exciting range of single site measurements including demonstrating aspects of quantum computing.[7–11,33,34,44,45] In the model adopted to interpret their results they have spin as a good quantum number and spin-orbit interaction is neglected. It is doubtful that spin-orbit can be totally neglected but it is small and there is a correspondence in the energy level schemes and selection rules between their work and that given here. There are also some similarities in the values of the parameters. For example, we have determined that the rate constant for intersystem crossing from the excited x',y' states to the singlet s has a value of $k_{x's}=k_{y's}=0.39\times 1/\tau$. This is in good correspondence with a value of $0.5\times 1/\tau$ given by Nizovtsev *et al.*[34] They have also proposed that there is much slower transfer from the $^3E\ z'$ state to the singlet and we agree with this conclusion. They have given a value of $k_{z's}=2.5\times 10^{-4}\times 1/\tau$. In our model it is considered to be zero but a small value such as they have given does not change the behavior of the system. There is, therefore, reasonable agreement when considering the populating of the singlet level. The situation for transfer out of the singlet level is different and there is some confusion. There is no agreement when the singlet is taken to have the long 0.275 s lifetime and when there is no decay from this singlet to the ground state.[34] In this situation the spin polarization and transfer out of the singlet has to be through thermal back transfer plus optically driven processes. However, these processes are not consistent with the optically induced spin polarization rate being independent of temperature and linear in excitation intensity.[24,43] As there are no such processes in our model there can be no comparison made with the parameters given. In other work[9,31,33,45] direct transfer from the singlet to the ground state is indicated and mention made of a short singlet lifetime.[45] No parameters are given to enable a comparison but clearly there is a consistency with the model presented here.

Jelezko *et al.*[9] have observed a single sharp zero-phonon line in the excitation spectrum of single centers. This is a very significant observation as it is crucial for readout for many NV quantum information processing applications. Detection requires there to be a transition that cycles without change of spin projection and their observation indicates that the $z\leftrightarrow z'$ transition can cycle $\sim 100\,000\times$ before the change occurs.[45] This is in contrast to that obtained by our model, where with present parameters, the cycling of the $z\leftrightarrow z'$ transition would be limited to $\sim 50\times$ before a change of spin state. In the model the cycling is limited by the non-spin-conserving optical transitions and, as noted earlier, the strength of these transitions vary with strain. Strain varies the separation of S_z and (S_x,S_y) spin levels and consequently the degree of mixing via the nonaxial spin-orbit interaction. This variation has been investigated experimentally by Santouri *et al.*[29] By studying small regions of an irradiated crystal they were able to obtain an inhomogeneous line width (15 GHz) orders of magnitude narrower than obtained previously. Changing the spacial location gave spectra for different magnitudes of strain and the ^3E splitting was resolved. Furthermore, clear hyperfine structure associated with the various optical transitions was obtained from two-laser hole burning measurements. Previous two-laser hole burning data indicated that the S_z spin state was lowest in both the lower and upper component of the strain-split ^3E state. This is confirmed in the recent hole burning measurements and it is shown that this is the case with even small strain splittings of <10 GHz. With such strain fields the order of the levels is, therefore, dominated by "spin-spin type" terms rather than by spin orbit. The effect of this interaction at zero strain in Fig. 1(a) is to displace the S_x,S_y states with respect to the S_z. This increases the spin separations in the upper branch and reduces the separation in the lower branch (or vice versa) and with increasing strain there will be a crossing of the spin levels in the lower energy branch [between Figs. 1(a) and 1(b)]. Thus, in the lower branch the levels are closer and give larger mixing of S_z and S_x,S_y spin states. Transitions to the lower branch are, therefore, conducive to hole burning and electromagnetic induced transparency[29] as both require non-spin conserving transitions. Alternatively transitions to the upper level are more favorable for cyclic transitions and with low strain such transitions may account for the very cyclic transitions observed by Jelezko *et al.*[9] An understanding of these processes and their variability require knowledge of the magnitude of the interactions associated with the ^3E excited state. This has not been obtained in detail and remains an outstanding issue for a full understanding of the electronic structure of the NV center.

VIII. CONCLUSION

In this work group theoretical considerations have been used to account for the electronic states of the NV center, for the optical transitions and for the intersystem crossing. The account leads to a seven level model where the dynamics are dominated by four rate constants. These four rate constants are determined from independent experimental measurements and it is shown that with the values obtained the model gives plausible correspondence with additional optical measurements of ensembles. The comparison between theory and experiment is not fully quantitative but the agreement is sufficient to give confidence in the appropriateness of the model. A good physical understanding of the response of the center to optical excitation is obtained and the significance is that the model provides a basis for the development of strategies to target the remaining outstanding issues regarding the properties of the NV center. The model also provides a sufficient understanding of the dynamics to allow for satisfactory development of many NV applications.

ACKNOWLEDGMENTS

The above work has been supported by a DARPA QuIST grant through Texas Engineering Experimental Station and by Australian Defence Science and Technology Organization. The authors thank Philip Hemmer (Texas A&M University) and Fedor Jelezko (University of Stuttgart) for useful discussions.

[1] A. Gruber, A. Drabenstedt, C. Tietz, L. Fleury, J. Wrachtrup, and C. von Borczyskowski, Science **276**, 2012 (1997).
[2] A. Drabenstedt, C. Tietz, F. Jelezko, J. Wrachtrup, S. Kilin, and A. Nizovtzev, Acta Phys. Pol. A **96**, 664 (1999).
[3] A. Drabenstedt, L. Fleury, C. Tietz, F. Jelezko, S. Kilin, A. Nizovtzev, and J. Wrachtrup, Phys. Rev. B **60**, 11 503 (1999).
[4] C. Kurtsiefer, S. Mayer, P. Zarda, and H. Weinfurter, Phys. Rev. Lett. **85**, 290 (2000).
[5] R. Brouri, A. Beveratos, J-Poizat, and Philippe Gragier, Opt. Lett. **25**, 1294 (2000); A. Beveratos, S. Kuhn, R. Brouri, T. Gacoin, J.-P. Poizat, and P. Grangier, Eur. Phys. J. D **18**, 191 (2002); A. Beveratos, R. Brouri, T. Gacoin, J.-P. Poizat, and P. Grangier, Phys. Rev. A **64**, 061802(R) (2002).
[6] A. Beveratos, R. Brouri, T. Gacoin, A. Villing, J.-P. Poizat, and P. Grangier, quant-ph/2061361 (unpublished); A. Beveratos, R. Brouri, J. P. Poizat, and P. Grangier, in *QCM and C 3 Proceedings*, edited by P. Tombesi (Kluwer Academic, Dordrecht, 2000), p. 261.
[7] J. Wrachtrup, S. Ya. Kilin, and A. P. Nizovtsev, Opt. Spectrosc. **91**, 429 (2001).
[8] F. Jelezko, I. Popa, A. Gruber, C. Tietz, J. Wrachtrup, A. Nizovtsev, and S. Kilin, Appl. Phys. Lett. **81**, 2160 (2002).
[9] F. Jelezko, T. Gaebel, I. Popa, M. Domhan, A. Gruber, and J. Wrachtrup, Phys. Rev. Lett. **93**, 130501 (2004).
[10] F. Jelezko and J. Wrachtrup, J. Phys.: Condens. Matter **16**, R1089 (2004).
[11] F. Jelezko, T. Gaebel, I. Popa, A. Gruber, and J. Wrachtrup, Phys. Rev. Lett. **92**, 076401 (2004).
[12] L. du Preez, Ph.D. thesis, University of the Witwatersrand, Johannesburg, 1965.
[13] G. Davies and M. F. Hamer, Proc. R. Soc. London, Ser. A **348**, 285 (1976).
[14] J. W. Steeds, S. Charles, T. J. Davis, A. Gilmore, J. Hayes, D. Pickford, and J. E. Pickford, Diamond Relat. Mater. **8**, 94 (1999).
[15] J. H. H. Loubser and J. A. van Wyk, Diamond Res. **1**, 11 (1977).
[16] N. R. S. Reddy, N. B. Manson, and C. Wei, J. Lumin. **38**, 46 (1987).
[17] E. van Oort, N. B. Manson, and M. Glasbeek, J. Phys. C **21**, 4385 (1988).
[18] D. A. Redman, S. Brown, R. H. Sands, and S. C. Rand, Phys. Rev. Lett. **67**, 3420 (1991).
[19] N. B. Manson, P. T. H. Fisk, and X.-F. He, Appl. Magn. Reson. **3**, 999 (1992).
[20] A. Lenef, S. W. Brown, D. A. Redman, S. C. Rand, J. Shigley, and E. Fritsch, Phys. Rev. B **53**, 13 427 (1996); A. Lenef and S. C. Rand, Phys. Rev. B **53**, 13441 (1996).
[21] J. P. Goss, R. Jones, P. R. Briddon, G. Davies, A. T. Collins, A. Mainwood, J. A. van Wyk, J. M. Baker, M. E. Newton, A. M. Stoneham, and S. C. Lawson, Phys. Rev. B **56**, 16031 (1997); A. Lenef and S. C. Rand, *ibid.* **56**, 16033 (1997).
[22] C. A. Coulson and M. J. Kersley, Proc. R. Soc. London, Ser. A **241**, 433 (1957).
[23] J. S. Griffith, *The Theory of Transition Metal Ions* (Cambridge University Press, Cambridge, 1961), p. 330.
[24] J. P. Harrison, M. J. Sellars, and N. B. Manson, J. Lumin. **107**, 245 (2004).
[25] J. Harrison, M. J. Sellars, and N. B. Manson, Diamond Relat. Mater. **15**, 586 (2006).
[26] R. T. Harley, M. J. Henderson, and R. M. Macfarlane, J. Phys. C **17**, L233 (1984).
[27] D. Redman, S. Brown, and S. C. Rand, J. Opt. Soc. Am. B **9**, 768 (1992).
[28] N. B. Manson and C. Wei, J. Lumin. **58**, 158 (1994).
[29] C. Santori, D. Fattal, S. M. Spillane, M. Fiorentino, R. G. Beausoleil, A. D. Greentree, P. Olivero, M. Draganski, J. R. Rabeau, P. Reichart, B. C. Gibson, S. Rubanov, D. N. Jamieson, and S. Prawer, Opt. Express **14**, 7986 (2006).
[30] J. P. D. Martin, J. Lumin. **81**, 237 (1999).
[31] A. P. Nizovtsev, S. Ya. Kilin, F. Jelezko, I. Popa, A. Gruber, and J. Wrachtrup, Physica B **340-342**, 106 (2003).
[32] J. P. Goss, R. Jones, S. J. Breuer, P. R. Briddon, and S. Oberg, Phys. Rev. Lett. **77**, 3041 (1996).
[33] A. P. Nizovtsev, S. Ya. Kilin, F. Jelezko, I. Popa, A. Gruber, C. Tietz, and J. Wrachtrup, Opt. Spectrosc. **94**, 848 (2003).
[34] A. P. Nizovtsev, S. Ya. Kilin, F. Jelezko, T. Gaelbal, I. Popa, A. Gruber, and J. Wrachtrup, Opt. Spectrosc. **99**, 233 (2005).
[35] G. Davies, J. Phys. C **7**, 3797 (1974).
[36] N. B. Manson and J. P. Harrison, Diamond Relat. Mater. **14**, 1705 (2005).
[37] T. Gaebel, M. Domhan, C. Wittmann, I. Popa, F. Jelezko, J. Rabeau, A. Greentree, S. Prawer, E. Trajkov, P. R. Hemmer, and J. Wrachtrup, Appl. Phys. B: Lasers Opt. **82**, 243 (2006).
[38] G. Davies, J. Phys. C **12**, 2551 (1979).
[39] A. T. Collins, M. F. Thomaz, and M. I. B. Jorge, J. Phys. C **16**, 2177 (1983).
[40] H. Hanzana, Y. Nisida, and T. Kato, Diamond Relat. Mater. **6**, 1595 (1997).
[41] F. Jelezko (private communication).
[42] F. Jelezko, T. Tietz, A. Gruber, I. Popa, A. Nizovtsev, S. Kilin, and J. Wrachtrup, Single Mol. **2**, 255 (2001).
[43] I. Hiromitsu, J. Westra, and M. Glasbeek, Phys. Rev. B **46**, 10600 (1992).
[44] I. Popa, T. Gaebel, M. Domhan, C. Wittmann, F. Jelezko, and J. Wrachtrup, Phys. Rev. B **70**, 201203(R) (2004).
[45] J. Wrachtrup and F. Jelezko, J. Phys.: Condens. Matter **18**, S807 (2006).